

Performance Enhanced In Reduction Of NO_x Emissions Using Swirl In A Combustion Procedure

Abdullah Alghafis*

*Mechanical Engineering Department, Unaizah Engineering College, Qassim University, Unaizah, KSA

Abstract

A numerical investigation of NO_x formation in natural gas-fired furnace is presented. In order to reduce NO_x emissions, a combustion modification technique is applied using the advantage of swirl in a non-premixed combustion process. As NO_x is produced at high temperatures, radiation needs to be included in this inquiry. The models of this study are selected of such kind there will be accurate computational results. The finite volume technique (FVM), paired with an extended eddy break-up model and the standard k- ϵ model, is developed to solve the radiative transfer equation (RTE). The thermal NO mechanism is used to predict the NO_x formation. It is clearly shown that swirl can reduce considerably the NO_x emission.

Keywords: swirl, NO_x emission, combustion, radiation.

Introduction

The NO_x is produced during combustion, especially at high temperatures. They present a contributor to air pollution and have dangerous effects to human health and environment such as destruction of stratospheric ozone by NO. For that reason, their reduction becomes a challenge. The major NO_x reduction techniques are: fuel switching, combustion control, fuel gas treatment and fuel reburning. Those techniques can be classified in two types: the post-combustion techniques such as selective catalytic reduction, and combustion modification technique. Particularly, swirl intensity is one of the important operating parameters which can be used in combustion control. This parameter is included in combustion modification techniques of NO_x emissions.

For the combustion systems, in the industry field, there are many research works and efforts to simultaneously increase combustion efficiency and decrease the soot formation and NO_x emissions. This subject becomes very important, nowadays, because of the increasing use of installations such as furnaces, boilers and gas turbines. According to Bowman (1992), there are four main ways that NO_x is produced: (a) the thermal NO mechanism; (b) the quick NO mechanism; (c) the NO_2 (nitrous oxide) method; and (d) the fuel-bound nitrogen mechanism. We discovered all four of these mechanisms in the literature. Actually, the first two systems influence the creation of NO. The main of this work is to show a reduction technique of NO_x emissions by combustion control using swirl.

II. Geometry and numerical scheme

II.1. Geometry

Axisymmetric, natural gas-fired whirling furnace known as the "Harwell furnace" is the system being explored and shown in Fig.1. So, we have a 2D axisymmetric problem.

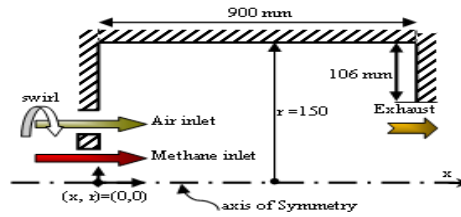


Fig. 1: Standard computational fluid dynamics (CFD) example, the so-called “Harwell furnace”: geometry and coordinate system (not to scale).

II.2. Numerical scheme

Using the two cylindrical coordinates x and r , a generalized form of the momentum equations is given as

$$\frac{1}{r} \left[\frac{\partial}{\partial x} (r \rho u r \phi) + \frac{\partial}{\partial r} (r \rho v r \phi) - \frac{\partial}{\partial x} (r \Gamma_{eff} \frac{\partial \phi}{\partial x}) - \frac{\partial}{\partial r} (r \Gamma_{eff} \frac{\partial \phi}{\partial r}) \right] = S_{\phi} \quad (1)$$

with ϕ denotes general dependent variables: the mixture fraction, enthalpy, the u and v components of velocity, the turbulent kinetic energy, and the turbulent dissipation rate. Further, ρ , Γ_{eff} and S_{ϕ} stand for density, effective diffusion coefficient and generalized source term corresponding to ϕ . Γ_{eff} is the result of adding the laminar and turbulent transport coefficients, interpreted as the effective viscosity for $\phi = u, v, w$ and the effective diffusivity for

$$\phi = h, Z, Y_i$$

$$\Gamma_{eff} = \frac{\mu_l}{\alpha_{\phi l}} + \frac{\mu_t}{\alpha_{\phi t}} \quad (2.a)$$

with

$$\mu_{eff} = \mu_l + \mu_t \quad (2.b)$$

Where, μ_l and μ_t represent respectively the laminar and the turbulent viscosity. $\alpha_{\phi l}$ and $\alpha_{\phi t}$ are the laminar and turbulent Prandtl number respectively, corresponding to variable ϕ .

Addition of a tangential component to the air injection results in the swirl. The swirl number, is perhaps the most frequently utilized parameter, SW , which is the ratio of axial flux of angular momentum to axial flux of linear momentum as described by Nemoda et al. (2005).

$$SW = \frac{2\pi \int w r \rho u r dr}{2\pi R \int u \rho u r dr} \quad (3)$$

Where, w signifies the tangential component of velocity. The degree of swirl strength is expressed as a swirl number in this study.

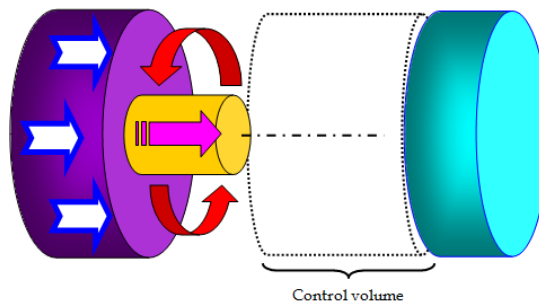


Fig. 2: Principle of a burner with swirl

II.2.1 Turbulence model

The turbulence closure is achieved by means of $k - \varepsilon$ model developed by Launder and Spalding (1974). The turbulence viscosity is determined by computing the distribution of turbulence energy and its dissipation rate by using the relationship

$$\mu_t = C_\mu \rho \frac{k^2}{\varepsilon} \tag{4}$$

The constants of this model are shown in Tab. 1.

The source terms of the quantities k and ε are respectively

$$S_k = \mu_t G - C_\mu \rho^2 k^2 / \mu_t \tag{5.a}$$

$$S_\varepsilon = C_{\varepsilon_1} G C_\mu \rho k - C_{\varepsilon_2} \frac{\rho \varepsilon^2}{k} \tag{5.b}$$

Where, G stands for the mean motion's output of turbulent kinetic energy, and it is represented by

$$G = 2 \left[\left(\frac{\partial u}{\partial x} \right)^2 + \left(\frac{\partial v}{\partial r} \right)^2 + \left(\frac{v}{r} \right)^2 \right] + \left(\frac{\partial u}{\partial r} + \frac{\partial v}{\partial x} \right)^2 + \left(\frac{\partial w}{\partial x} \right)^2 + \left[r \frac{\partial}{\partial r} \left(\frac{w}{r} \right) \right]^2 \tag{6}$$

C_μ	C_{ε_1}	C_{ε_2}	σ_k	σ_ε
0.09	1.44	1.92	1.0	$\frac{K^2}{(C_{\varepsilon_2} - C_{\varepsilon_1}) \sqrt{C_\mu}}$

Tab. 1: Constants of the standard $k-\varepsilon$ model

with the Van-Karman constant $K=0.4187$.

Due to viscous effects, the typical $k-\varepsilon$ model, which is a high-Reynolds model, cannot be used in the area close to the wall. So, to handle the area next to the wall, we applied the wall function described by Launder and Spalding (1974).

II.2.2 Combustion model

Methane-air reaction in one step combustion can be described by the global reaction below



The eddy break-up model is restricted by the fact that the reaction rate is independent of the local chemistry and that the flow does not account for the transport of the turbulent flame. For that reason, in this paper, an advanced eddy break-up model, developed by Mantel and Borghi (1994), is used. The equation below provides the mean reaction rate.

$$\bar{w} = \rho C_{EBU} \frac{\bar{Y}(Y_0 - \bar{Y})}{\tau_t} \tag{7.a}$$

Where,

$$C_{EBU} = \frac{\alpha_0 \left(1 + c \frac{U_L}{u'} \right)^{2\gamma}}{\beta_0 Y_0 \left(\frac{1}{2} - b_0 \right)} \tag{7.b}$$

By using the ratio u'/U_L , the model considers how chemistry and turbulence interact.

II.2.3 NO_x formation model

Nitric oxide (NO) and nitrogen oxide (NO₂) are referred to as "NO_x." In fact, the total NO_x emission consists of 95% NO (5% is NO₂). Additionally, the two pathways, prompt NO route and thermal NO route predominate the NO production process. But, the prompt mechanism, which was postulated by Fenimore (1979), only

contributes a little portion of the overall NOx. That is why, in this paper, the Zeldovich mechanism (1946) of thermal NO generation is the only one used to explain how NO is formed.



With those considerations, when the NOx generation rate is given by only the NO species transport equation (Eq 1) is necessary.

$$\frac{d[NO]}{dt} = k_{+1}[N_2][O] + k_{+2}[N][O_2] - k_{-1}[NO][N] - k_{-2}[NO][O] \quad (8)$$

If the N atom is approximated by a steady state, where it is generated as quickly as it is destroyed, we get

$$\frac{d[N]}{dt} = k_{+1}[N_2][O] - k_{+2}[N][O_2] = 0 \quad (9)$$

Placed in Eq. (8), this gives

$$\frac{d[NO]}{dt} = 2k_{+1}[N_2][O] \quad (10)$$

To solve the transport equation for the case $\phi = Y_{NO}$ (see Eq. (1)), the source term is written as

$$S_{NO} = 2\rho k_{+1} Y_{N_2} [O] M_{NO} / M_{N_2} \quad (11)$$

Where, $M_{NO} = 30\text{g/mol}$, is NO molecular mass, $M_{N_2} = 28\text{ g/mol}$, is N_2 molecular mass, and, $k_{+1} = 1.8 \cdot 10^8 e^{-38370/T}$. The O_2 and N_2 concentrations are obtained from combustion solution. Thereafter, according to Skjøth-Rasmussen et al. (2004), the O-atom concentration, [O], may be deduced from the below mentioned expression

$$[O] = AT^B \exp\left(\frac{E}{RT}\right) [O_2]^{0.5} \quad (12)$$

where, the gas constant is $R=8.314$ and the reaction activation energy is E, A and B are two variables in the above expression. The O-atom model, which can increase the rate of NO production in the reacting area, is described as Jiang et al. (2006)

$$[O] = 3.97 \times 10^5 T^{-0.5} [O_2]^{0.5} \exp\left(\frac{-31090}{T}\right) \quad (13)$$

II.2.4 Radiation

To solve the RTE, we used the FVM by Gassoumi et al (2009). Particularly, in this work, we consider a non-gray soothing media. So, RTE can be expressed as follows in an absorbing-emitting and scattering grey medium:

$$\begin{aligned} (\vec{\Omega} \cdot \vec{\nabla}) I_\nu(\vec{r}, \vec{\Omega}) &= \kappa_\nu(\vec{r}) I_b(\vec{r}) - \beta_\nu(\vec{r}) I(\vec{r}, \vec{\Omega}) + \\ &\frac{\sigma_{s\nu}(\vec{r})}{4\pi} \int_{\Omega=4\pi} \Phi_\nu(\vec{\Omega}' \rightarrow \vec{\Omega}) I_\nu(\vec{r}, \vec{\Omega}') d\Omega' \end{aligned} \quad (14)$$

The extinction, β_ν scattering, $\sigma_{s\nu}$ and absorption κ_ν coefficients all rely on frequency ν in non-gray media. $I_\nu(\vec{r}, \vec{\Omega})$ is the spectral radiation intensity at any position \vec{r} and along a direction $\vec{\Omega}$. $I_{b\nu}$ is the spectral blackbody radiation intensity. $\Phi_\nu(\vec{\Omega}' \rightarrow \vec{\Omega})$ depicts the phase function of spectral scattering from the entering direction $\vec{\Omega}'$ to the departing direction $\vec{\Omega}$. Particularly, in the opinion of Liu et al. (2000), the spatial derivative component in Eq. 14 in the cylindrical coordinates for a two-dimensional axisymmetric issue is

$$(\vec{\Omega} \cdot \vec{\nabla}) I(\vec{r}, \vec{\Omega}) = \frac{\mu}{r} \frac{\partial(I)}{\partial r} - \frac{1}{r} \frac{\partial(\eta I)}{\partial \Psi} + \xi \frac{\partial I}{\partial x} \quad (15)$$

where μ , η and ξ are the direction cosines, and Ψ is the azimuthal angle calculated from the direction. According to Kim and Baek (2003), whenever we consider the cylindrical coordinates, the RTE is a function of spatial two-dimensions (x, r) and two coordinates (θ, Ψ) and it is given by

$$\frac{\mu^{mn}}{r} \frac{\partial}{\partial r} (r I^{mn}) - \frac{1}{r} \frac{\partial (\eta^{mn} I^{mn})}{\partial \Psi} + \xi^{mn} \frac{\partial I^{mn}}{\partial z} = -(\kappa + \sigma_s) I^{mn} + S_R^{mn} \quad (16)$$

The direction cosines are defined by

$$\begin{cases} \mu^{mn} = \sin \theta \cos \Psi & (17.a) \\ \eta^{mn} = \sin \theta \sin \Psi & (17.b) \\ \xi^{mn} = \cos \theta & (17.c) \end{cases}$$

and the direction is written as

$$\Omega^{mn} = (\mu^{mn}, \eta^{mn}, \xi^{mn}) \quad (18)$$

III. Results and discussions

In this study, the possibility to reduce NO_x emissions is numerically investigated in depth in a standard computational fluid dynamic (CFD) example, the cylindrical structure known as the "Harwell furnace". The experiment setup and inlet conditions are mentioned in Tab. 2 which is provided by Wilkes et al. (1989).

The swirl creates two kinds of recirculation zone: a central toroidal recirculation zone (CTRZ) due to vortex disruption and a corner recirculation zone (CRZ) brought on by the abrupt expansion of the combustor design. The ensuing vortex activity will cause a low-pressure area to form along the chamber's axis. Sometimes short tangential chutes in the flame-tube rather than plain apertures are used to inject the secondary air, which enhances the vortex motion. The temperature distribution depends on the swirl number, in the other hand on the mixing fuel-air. In addition, according to the swirl level, we can obtain a good mixing. So, it is possible to control flame stabilization and reduce the NO_x emissions when swirl is applied.

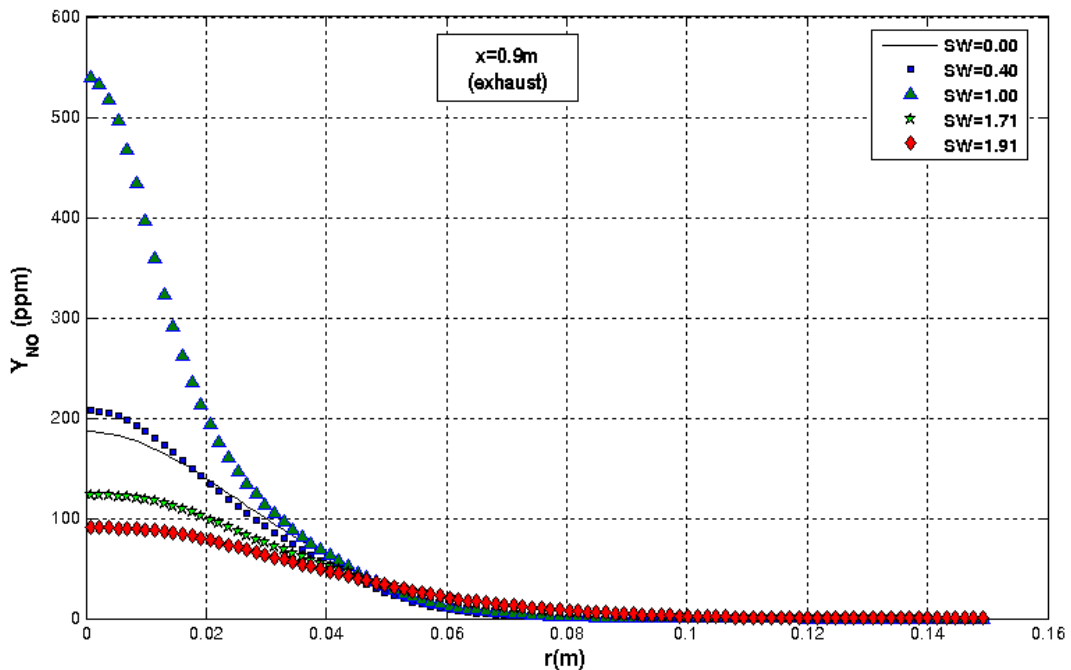


Fig. 3: NO mass fraction as a function of swirl number at the exhaust of the furnace.

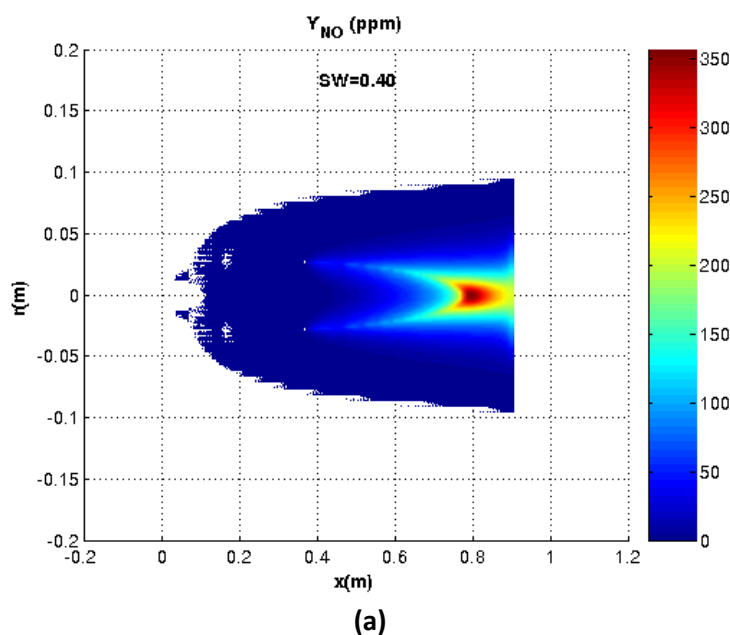
Figure 3 depicts the variation of NO_x emissions as function of swirl number. Generally, temperature increases with increased swirl intensity level because the rate of reaction increases due to the good mixing offered.

Fuel intake zone (mm)	<i>from r=0.0 to r=6.0</i>	
Air intake zone (mm)	<i>from r=13.5 to r=27.5</i>	
Furnace diameter (mm)	150.0	
Length of furnace (mm)	900.0	
Intake conditions	fuel	air
axial velocity (m/s)	15.0	12.8
radial velocity (m/s)	0.0	0.0
turbulent kinetic energy $k(m/s^2)$	2.26	1.63
dissipation rate of turbulence ϵ (m/s)	1131.8	692.0
temperature (K)	295	295
swirl number	0.0	0.4
mass fraction of O₂	0.0	0.2315
mass fraction of N₂	0.0	0.7685
mass fraction of CH₄	1.0	0.0
Heat of reaction (MJ/kg)	45.5	

Tab. 2: Experiment setup and inlet conditions

There are two cases when swirl is applied: an interval of SW, where the NO mass fraction, Y_{NO} , increases with the swirl number, SW, and case (2) an interval, where Y_{NO} decreases. In the first case, from SW=0 (without swirl) to SW=1, Y_{NO} increases considerably. For swirl situation, the NOx content is higher. Additionally, compared to non-swirl cases, swirl case increases the rate of NOx generation.

But, in the second case, there is an optimal and an adequate value of SW from which NO_x emissions decrease. There is a turning point occurs at this stage where the NO_x emissions decrease. At the exhaust, as it is shown in Fig.3, for SW=1.71, a 40,73% reduction in NO_x emission compared to SW=0.4 is obtained. For SW=1.91, the reduction becomes 56.36%. The reduction tendency can be seen clearly in Fig.3. The illustration shows clearly that increasing enough SW, the NO_x formation will decrease. But we must note that the choice of SW is limited, because a high level can cause: (a) the detachment of the flame, (b) flame quenching, and (c) flame flash-back to the fuel injection zone.



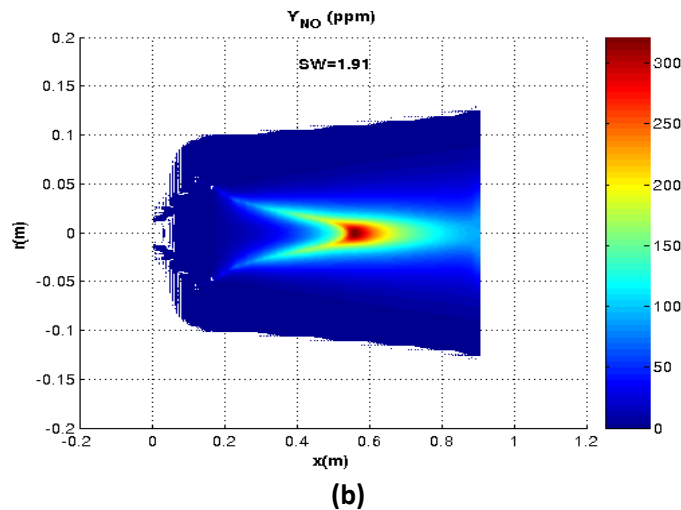


Fig. 4: NO mass fraction distributions: case (a) SW=0.4, and (b) SW=1.91, a 14.29% reduction in NO_x emissions from (a) to (b).

Generally, Higher rates of entrainment and quick mixing from swirling increase flame stability and shorten flame length. A 28% reduction in flame length clearly observed in our case. Figure 4 illustrates the NO mass fraction distributions for two swirl number. It is clearly shown that due to the intense recirculation, NO is reduced via reactions with hydrocarbon and hydrocarbon intermediates such HCN, similar to those involved in Fenimore mechanism (1979). The reburning fuel can be achieved when an important quantity of gases go back to the injection zone. In fact, swirl increases significantly the convective exchange and the recirculation zones of fluid dominate the media when swirl number becomes important. Completely, NO_x reductions of 14.29% have been recorded (see Fig. 4). shear layer region, which improve flame stability.

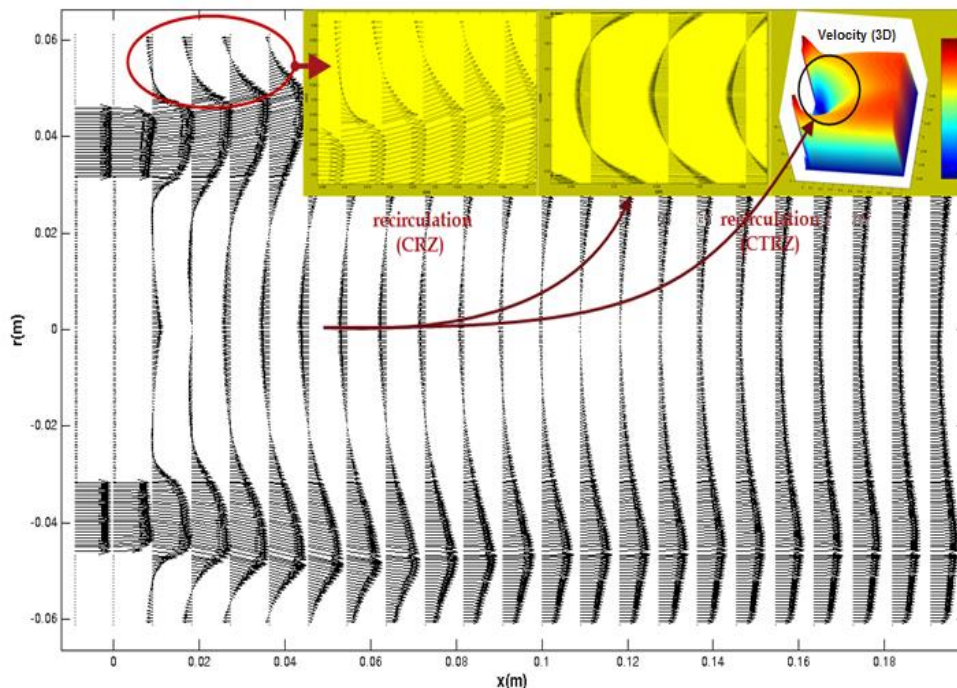


Fig. 5: Velocity distribution and the different recirculation zones.

This outcome demonstrated that swirl does assist in combining the fuel and air ahead of combustion, reducing NO_x emissions. However, this was achieved at the expense of reduction in combustion stability. We can conclude that, When the optimal setting is chosen, the swirl's effect on NO_x emissions becomes larger. In addition, the best choice of the radiative properties of burner and combustor wall surfaces reduce considerably the burned gas temperature which in turn results in low formation by the thermal NO. For this reason, radiation needs to be considered in combustion devices that operate at high temperatures.

IV. Conclusion

This manuscript gives a method to reduce NO_x emission in swirling combustion systems. Reduction of NO_x emissions by up to 14.29% has been recorded from a breaking value of swirl number. In fact, swirl is a factor of importance which enables an excellent blending of the mixture when all the fuel injected can be burned by ensuring a good mixing. An important heat convective exchange can be added to the radiative transfer if swirl becomes important. In fact, the swirl number must be selected with a compromise between combustion stability and NO_x emission to reduce the later and, consequently, protect human health and the global environment from their great threat and detrimental effects.

Symbols/notations

u, v	: axial and radial velocity component, respectively [$\text{m}\cdot\text{s}^{-1}$]
I	: radiant intensity [$\text{W}\cdot\text{m}^{-2}\cdot\text{sr}^{-1}$]
k	: turbulent energy [$\text{m}^2\cdot\text{s}^{-2}$]
S	: source term
T	: Temperature [K]
G	: production term of turbulent kinetic energy
SW	: swirl number
ε^w	: wall emissivity
x, r	: co-ordinate axes in cylindrical geometry
Y	: Mass fraction [ppm]
$[i]$: concentrations of species i [$\text{mol}\cdot\text{m}^{-3}$]
<i>Greek letters</i>	
β	: extinction coefficient = $\kappa + \sigma$ [m^{-1}]
ε	: dissipation rate of energy [$\text{m}^2\cdot\text{s}^{-3}$]
ϕ	: general dependent variable
μ	: viscosity [$\text{kg}\cdot\text{m}^{-1}\cdot\text{s}^{-1}$]
ρ	: density [$\text{kg}\cdot\text{m}^{-3}$]
$k_{+1}, k_{-1}, k_{+2}, k_{-2}$: Rate constants for the reactions (R2) [$\text{m}^3\cdot\text{mol}^{-1}\cdot\text{s}^{-1}$]
<i>Subscripts</i>	
NO	: Nitric oxide
eff	: Effective exchange coefficient
t	: turbulent transport coefficient
l	: Laminar transport coefficient
$+, -$: Forward and backward reaction respectively
<i>Superscripts</i>	
w	: wall

Conflicts of Interest

This is to assure that there is no any type of conflict of interest in publication of original research work done.

References

1. Bowman C. T., Control of combustion-generated nitrogen oxide emissions: Technology driven by regulation, in: 24th Symposium (International) on Combustion, The Combustion Institute, 859–878, (1992).
2. Fenimore C. P., Studies of fuel-nitrogen species in rich flame gases, in: 17th Symposium (International) on Combustion, The combustion institute, Philadelphia, PA, 661–670, (1979).
3. Gassoumi T., Guedri K., and Said R., Numerical study of the swirl effect on a coaxial jet combustor flame including radiative heat transfer, Numerical Heat Transfer, Part A, 56: 897–913, (2009).

4. JIANG B., LIANG H., HUANG G., and LI X., Study on NO_x formation in CH₄/air jet combustion, Chinese Journal of Chemical Engineering, Vol.14, 723-728, (2006).
5. Kim M.Y. and Baek S.W., Modeling of radiative heat transfer in an axisymmetric cylindrical enclosure with participating medium, Journal of Quantitative Spectroscopy & Radiative Transfer, Vol. 90, 377–388, (2005).
6. Launder B. E. and D. B. Spalding, Mathemaical Models of Turbulence, Academic Press, New York, 1972.
7. Liu J., Shang H. M. and Chen Y. S., Development of an unstructured radiation model applicable for two-dimensional planar, axisymmetric, and three-dimensional geometries, Journal of Quantitative Spectroscopy & Radiative Transfer, Vol. 66, 17-3, (2000).
8. Mantel T., Borghi R., A new model of premixed wrinkled flame propagation based on a scalar dissipation equation, Combustion and Flame, Vol. 96, 443–457, (1994).
9. Nemoda S., Bakic V., Oka S., Zivkovic G., and Crnomarkovic N., Experimental and numerical investigation of gaseous fuel combustion in swirl chamber, Inter. J. Heat and Mass Transfer, Vol. 48, 4623–4632, (2005).
10. Skjøth-Rasmussen, M.S., Glarborg, P., Østberg, M., Johannessen, J.T., Livbjerg, H. Jensen, A.D., Christensen, T.S., Formation of polycyclic aromatic hydrocarbons and soot in fuel-rich oxidation of methane in a laminar flow reactor, Combustion and Flame, Vol. 136, 91-128, (2004).
11. Wilkes N.S., Guilbert P.W., Shepherd C.M., Simcox S., The application of HARWELL-FLOW3D to combustion models, AERE-R13508, in: Atomic Energy Authority Report, Harwell, UK, (1989).
12. Zeldovich J., The oxidation of nitrogen combustion and explosions, Acta Physicochim, URSS 21, 577–628, (1946).